

Dihydrogen-Driven NADPH Recycling in Imine Reduction and P450-Catalyzed Oxidations Mediated by an Engineered O₂-Tolerant Hydrogenase

Janina Preissler,^[a] Holly A. Reeve,^{*,[b]} Tianze Zhu,^[b] Jake Nicholson,^[b] Kouji Urata,^[b] Lars Lauterbach,^{*,[a]} Luet L. Wong,^[b] Kylie A. Vincent,^{*,[b]} and Oliver Lenz^{*,[a]}

The O₂-tolerant NAD⁺-reducing hydrogenase (SH) from *Ralstonia eutropha* (*Cupriavidus necator*) has already been applied *in vitro* and *in vivo* for H₂-driven NADH recycling in coupled enzymatic reactions with various NADH-dependent oxidoreductases. To expand the scope for application in NADPH-dependent biocatalysis, we introduced changes in the NAD⁺-binding pocket of the enzyme by rational mutagenesis, and generated a variant with significantly higher affinity for NADP⁺ than for the natural substrate NAD⁺, while retaining native O₂-tolerance. The

applicability of the SH variant in H₂-driven NADPH supply was demonstrated by the full conversion of 2-methyl-1-pyrroline into a single enantiomer of 2-methylpyrrolidine catalysed by a stereoselective imine reductase. In an even more challenging reaction, the SH supported a cytochrome P450 monooxygenase for the oxidation of octane under safe H₂/O₂ mixtures. Thus, the re-designed SH represents a versatile platform for atom-efficient, H₂-driven cofactor recycling in biotransformations involving NADPH-dependent oxidoreductases.

Introduction

Biocatalysis is becoming established as a valuable tool in the production of complex chemicals.^[1] In particular biocatalytic transformations for asymmetric reductions including ketone, alkene and imine reductions, and for controlled oxidations such as terminal alcohol to aldehyde conversions and C–H bond activations, are becoming accepted as promising alternatives to traditional chemical methods.^[2] However, the enzymes that catalyze these transformations rely on electron transfer to or from redox equivalents which in most cases are the expensive biological cofactors NAD(P)⁺ or NAD(P)H.^[3] To develop viable biocatalytic processes, it is essential to have efficient systems for recycling these cofactors.

One of the most commonly used cofactor recycling systems for NAD(P)H is glucose-(6P) dehydrogenase which reduces NAD(P)⁺ at the expense of glucose-(6P) oxidation.^[4] The gluconolactone thus formed spontaneously hydrolyses to gluconic acid, rendering the reaction irreversible and leads to acidification of the reaction solution, which necessitates continuous pH monitoring and adjustment. The large quantity of gluconic acid waste also lowers the atom efficiency of the reaction, complicates recovery of water-soluble products and limits the potential environmental benefits of biocatalysis. Alternative systems for cofactor recycling are phosphite dehydrogenase and alcohol dehydrogenase, which, however, produce phosphate and aldehydes/ketones, respectively, as unwanted by-products during NAD(P)H recycling.^[5] Formate dehydrogenase (FDH) represents another widely used cofactor regeneration system. FDH couples NAD(P)⁺ reduction with the oxidation of formate, but also suffers from low enzymatic activity and formation of the by-product CO₂.^[6]

In contrast, the use of H₂ gas as a source of reducing equivalents allows atom-efficient recycling of NAD(P)H without any by-product that may alter the pH or complicate product recovery.^[7] Indeed, two different NAD(P)⁺-linked soluble hydrogenases (SHs) have been demonstrated for H₂-driven NADH or NADPH recycling to support the activity of a range of NAD(P)H-dependent enzymes.^[8,9] One of them is the archaeal NADP⁺-linked [NiFe]-hydrogenase (I) from *Pyrococcus furiosus* (PfSHI), which works well in a wide temperature range of 30–80 °C and reduces NADP⁺ rather than NAD⁺. Although described as partially O₂-tolerant,^[10] electrochemical measurements on PfSHI at 60 °C, show that the H₂ oxidation activity of the enzyme at 1 bar H₂ drops rapidly when 1 % O₂ is introduced, settling at a level corresponding to about 8 % of the anaerobic activity, while at 25 °C the activity drops to zero under 1 % O₂.^[11] Sustained H₂-driven NADP⁺ reduction in the presence of O₂ has

[a] Dr. J. Preissler, Dr. L. Lauterbach, Dr. O. Lenz
Institute of Chemistry, Biophysical Chemistry
Technische Universität Berlin
Straße des 17. Juni 135
10623 Berlin (Germany)
E-mail: lars.lauterbach@tu-berlin.de
oliver.lenz@tu-berlin.de

[b] Dr. H. A. Reeve, Dr. T. Zhu, J. Nicholson, Dr. K. Urata, Prof. L. L. Wong,
Prof. K. A. Vincent
Department of Chemistry
University of Oxford
Inorganic Chemistry Laboratory
South Parks Road
Oxford, OX1 3QR (UK)
E-mail: holly.reeve@chem.ox.ac.uk
kylie.vincent@chem.ox.ac.uk

Supporting information for this article is available on the WWW under <https://doi.org/10.1002/cctc.202000763>

© 2020 The Authors. Published by Wiley-VCH GmbH. This is an open access article under the terms of the Creative Commons Attribution License, which permits use, distribution and reproduction in any medium, provided the original work is properly cited.

not been demonstrated for *Pf*SHI. The O_2 sensitivity of the *Pf* enzyme represents a major drawback for hydrogenase-linked cofactor recycling as reactions need to be carried out under anaerobic conditions. It clearly cannot support cofactor supply for O_2 -dependent enzymes such as monooxygenases that utilise NAD(P)H to supply electrons for reductive activation of O_2 for oxygen atom insertion into C–H or C–C bonds.^[3,12,13]

The second promising candidate for both *in vitro*^[9,14] and *in vivo* cofactor recycling^[15] is the soluble NAD^+ -reducing [NiFe]-hydrogenase from *Ralstonia eutropha* (*ReSH*; *R. eutropha* is also known as *Cupriavidus necator*^[16]) which is able to catalyze H_2 -driven NAD^+ reduction even in the presence of ambient O_2 .^[17,18] Whole cells of *Pseudomonas putida* engineered to heterologously co-produce both the NADH- and O_2 -dependent P450 monooxygenase (CYP153A) from *Polaromonas* sp. JS666 and the *ReSH* were shown to oxidise octane to 1-octanol.^[15] However, many P450 enzymes of biotechnological interest are dependent on the phosphorylated derivative of NADH, NADPH. The *ReSH* is highly specific for NAD^+ , and H_2 -driven $NADP^+$ reduction by *ReSH* is not detected.^[19] Thus, the native enzyme is unsuitable for application in NADPH recycling and there have been no reports of isolated hydrogenases suitable for $NADP^+$ reduction in the presence of O_2 .

Since NADPH is generally less stable^[20] and more expensive than NADH there have been many reports, dating back to 1990, on changing the cofactor specificity of technologically useful enzymes from NADPH to NADH.^[21] There have been some notable successes, including structure-guided, semi-rational strategies for reversing nicotinamide cofactor specificity, as summarised by Cahn and coworkers.^[22] However, significant loss of catalytic activity tends to occur on attempting to alter cofactor selectivity and the need to engineer each oxidoreductase individually represents a significant burden. Thus, there is a clear need for improved O_2 -tolerant NADPH cofactor recycling systems that operate with high atom economy and high activity to support NADPH-dependent reductases and monooxygenases.

Here, we describe site-directed amino acid exchanges in *ReSH* which resulted in synthetic H_2 -dependent $NADP^+$ reduction activity which was still O_2 tolerant. The nicotinamide cofactor binding site of the *ReSH* is part of a non-classical Rossmann fold including a flavin mononucleotide (FMN). This arrangement is similar to that in the orthologous counterparts of respiratory Complex I, certain FDH enzymes, and [FeFe]-hydrogenases.^[23,24] During H_2 -driven NAD^+ reduction by the *ReSH*, the FMN accumulates two electrons, which are subsequently transferred as a hydride to NAD^+ resulting in the reduced form, NADH.^[25] In order to convert *ReSH* into a $NADP^+$ -reducing enzyme, we first constructed a homology model for the NAD(H)-binding subunit, HoxF, to identify promising sites for amino acid exchanges. This homology model is based on the crystal structure of the Nqo1 subunit from Complex I of *Thermus thermophilus*. A glutamate residue in the NADH-binding pocket of the corresponding subunit in Complex I from *E. coli* has been described to be crucial for cofactor specificity.^[26] We used this observation to modify the HoxF subunit of *ReSH* towards $NADP^+$ binding. Furthermore, classical Rossmann

motifs involved in nicotinamide cofactor binding have already been targeted to change cofactor specificity in many different dehydrogenases.^[22] For example, Lerchner et al. showed that by removing a positively charged residue, the $NADP^+$ -specific alcohol dehydrogenase from *Ralstonia* sp. was able to efficiently accept NAD^+ .^[27] Here, we used these findings to rationally design NADPH recycling SH variants that are able to support a stereoselective imine reductase and an octane-oxidising P450_{BM3} monooxygenase (CYP102A1).^[28] The latter case represents the first example of H_2 -driven NADPH recycling to support an O_2 -dependent biocatalytic process.

Results and Discussion

Construction of $NADP^+$ -reducing SH variants by rational design

Altering substrate specificity of NAD^+ -reducing SH by rational design required the identification of amino acid residues that are involved in substrate binding. Unfortunately, a crystal structure of SH from *R. eutropha* H16 is not yet available. The structure for the closely related SH from *Hydrogenophilus thermoluteolus* has been reported,^[29] which, however, does not contain the NAD(H) cofactor, whose precise orientation is essential for rational design of the corresponding binding pocket. Therefore, we used two crystal structures of Complex I from *Thermus thermophilus* (PDB accession numbers 2FUG and 3IAM) as templates for homology modelling (SWISS-MODEL) of HoxF (Figure 1a).^[30,31] The Nqo1 subunit of Complex I shows 62% sequence similarity with the C-terminal part of the HoxF subunit of *ReSH* (Figure S1) and, more importantly, has been crystallised in the presence of NADH.^[30] In the homology model, the NADH binding site (Figure 1b) is located in an unusual Rossmann fold featuring a glycine-rich loop that facilitates simultaneous binding of NADH and FMN.^[31] Stacking interactions between the nicotinamide ring of NADH and the isoalloxazine moiety of FMN as well as aromatic side chains of conserved amino acid residues guarantee precise cofactor positioning (Figure 1c). Several hydrogen bonds are formed between NADH and the protein backbone. One of these is formed between the carboxyl group of Glu341 and the 2'-hydroxyl group of the adenosine ribose of NADH (Figure 1c). In the case of NADPH, this hydroxyl group is replaced by a bulky, negatively charged phosphate group (Figure 1d), which would result in a steric clash with Glu341. Notably, this glutamate residue is absent in NADPH-specific dehydrogenases. We decided to engineer the specificity of the SH towards $NADP^+$ by exchanging Glu341, which interacts with NADH, for the smaller alanine residue (E341A), to allow accommodation of the $NADP^+$ -specific phosphate group. In NADP(H)-converting enzymes, a positively charged arginine is found in the neighbouring position to the alanine and stabilises NADP(H) binding by forming an ionic bond to the negatively charged phosphate group.^[22] We thus replaced Ser342 of the SH with an arginine (S342R, Figure 1d) to counterbalance the negatively charged phosphate group of NADPH. Construction of a single S342R

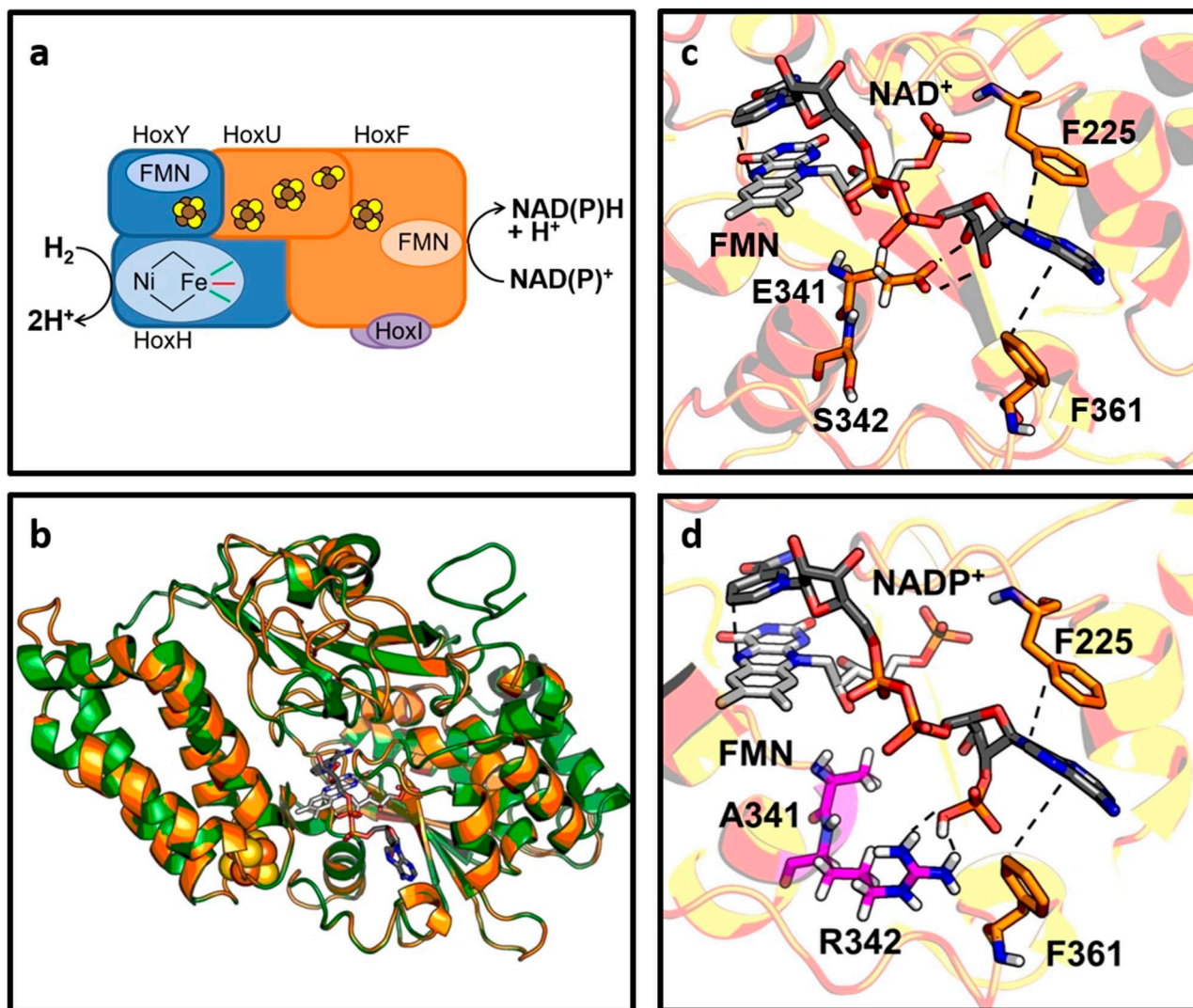


Figure 1. Subunit and cofactor composition of the soluble NAD^+ -reducing [NiFe]-hydrogenase (SH) of *R. eutropha* H16. (a) Schematic representation of the hydrogenase module (HoxH and HoxY subunits in blue) and the NAD^+ -reductase module (HoxF and HoxU subunits in orange). The latter carries two copies of the non-essential HoxI subunit. The iron-sulphur cluster relay connecting the two catalytic centres of the SH is shown as spheres. (b) Homology model of the HoxF subunit (orange) based on the crystal structure of the Nqo1 subunit (green) of Complex 1 from *Thermus thermophilus* (2FUG).^[31,34] The flavin mononucleotide and NADH molecules (shown as sticks) are taken from pdb entry 3IAM. (c) The NAD(H)-binding pocket of native SH. Important hydrogen bonding and π -stacking interactions are shown as dashed lines. (d) Model of the NAD(P)(H) binding pocket of the $\text{SH}^{\text{E341A/S342R}}$ variant (carbon atoms of exchanged amino acids in pink). Note the stabilising effect of the guanidinium group of R342 on the additional phosphate group of NADP^+ . The location of residue D467 is depicted in Figure S2.

variant was not considered because neighbouring negatively charged (D,E) and positively charged (R,K) residues were not observed in the cofactor binding site of any NAD(P)(H)-converting enzyme.^[32]

Finally, we considered amino acid residues, which do not directly interact with the cofactor, but contribute to overall charge of the binding pocket. The *R. eutropha* SH possesses a surface-exposed, negatively charged aspartate residue at position 467 (Figure S2), while the cyanobacterial soluble hydrogenases, which are reported to interact with both NADH and NADPH, carry either serine or threonine at the corresponding position^[33] (Figure S1). In order to assist NADP^+ binding, a D467S exchange was also introduced in the SH. The corresponding HoxF variants E341A, D467S, E341A/D467S, E341A/

S342R, and E341A/S342R/D467S were constructed by genetic engineering, and the resulting variant SH proteins, henceforth designated SH^{E467A} , $\text{SH}^{\text{E341A/D467S}}$, etc., were purified as described in the Experimental Section.

Biochemical and electrochemical properties of SH variants

First we measured the H_2 -dependent NAD(P)^+ reductase activities with 1 mM NAD(P)^+ at pH 8. As shown in Figure 2a, all the SH variants showed a dramatic decrease in H_2 -driven NAD^+ reduction activity (orange bars). The lowest activity was measured for the SH^{E341A} protein, with only 10% of the activity of native SH. However, NADP^+ reduction activity was already

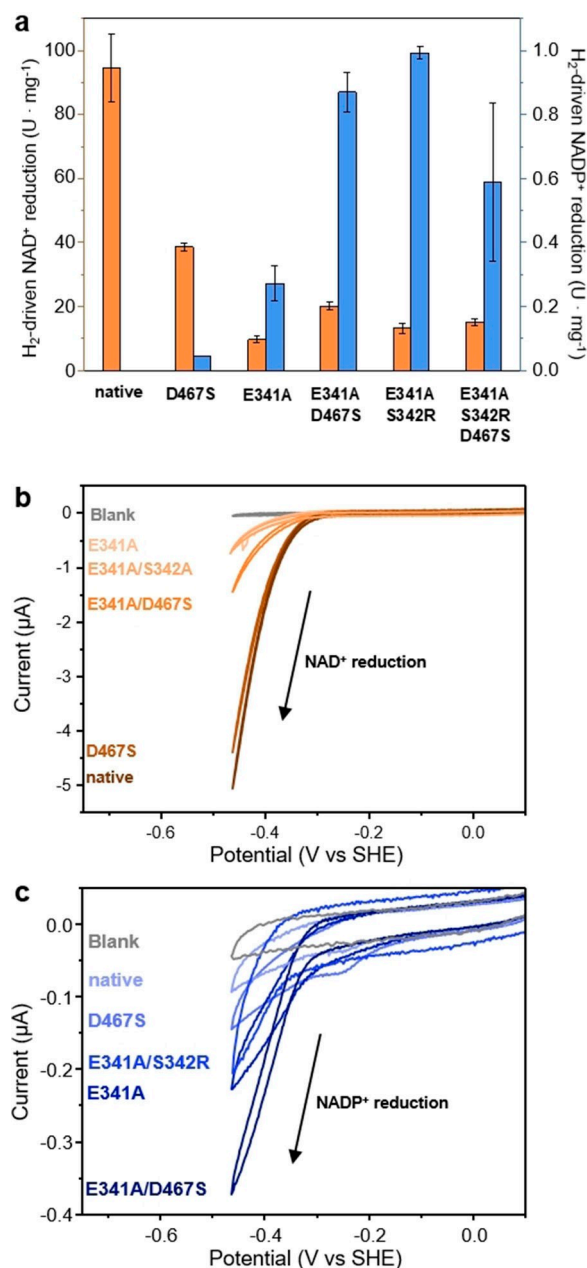


Figure 2. Comparison of the activity of the SH variants for NAD⁺ and NADP⁺ reduction. (a) Spectrophotometric determination of the H₂-driven NAD⁺ (orange) and NADP⁺ (blue) reduction activity. Conditions: 50 mM Tris-HCl buffer, pH 8, 1 mM NAD(P)⁺, 1 μM FMN and 1 mM dithiothreitol (DTT), 30 °C. H₂-dependent NADP⁺ reduction was not detectable for native SH. Means and error bars (calculated standard deviation) are derived from three biological replicates which were measured at least twice. In the case of NADP⁺ reduction by the SH^{D467S} variant the error bar is too small to be visible. (b) Electrode-driven NAD⁺ and, (c) NADP⁺ reduction activity measured at an enzyme-modified pyrolytic graphite electrode, rotated at 2000 rpm. Conditions: 100 mM Tris-HCl buffer, pH 8.0, 5 mM cofactor, scan rate 10 mV s⁻¹, 30 °C.

clearly detectable for this variant, which was not the case for the native SH. The NADP⁺ reduction activity increased in the order SH < SH^{D467S} < SH^{E341A} < SH^{E341A/D467S} < SH^{E341A/S342R} (Figure 2a). The NADP⁺ reduction activity of the SH^{E341A/S342R} variant

of 1 U · mg⁻¹ represents approximately 10% of the NAD⁺ reduction activity of this variant, and approximately 1% of the NAD⁺ reduction activity of native SH. The pH optimum of 7.5 of the NADP⁺ reduction activity of SH^{E341A/S342R} was found to be slightly lower than that (pH 8.0) for NAD⁺ reduction. Since all three exchanges had a positive effect on the NADP⁺ reduction of the SH, we combined them in a SH^{E341A/S342R/D467S} variant. This variant, however, showed a significantly lower NADP⁺ reduction activity than the two double exchange variants (Figure 2a). The low activity might be due to structural distortions of the cofactor binding site. The SH^{E341A/S342R/D467S} variant was therefore disregarded for the subsequent experiments.

Next, the NAD(P)⁺ reduction activity was determined electrochemically by means of protein film voltammetry. This method allows analysis of the NAD(P)⁺/NAD(P)H cycling moiety independently of the H⁺/H₂ cycling module and relies on interfacial electron transfer between the electrode and the immobilised enzyme. The activity of the enzyme film is proportional to the current, but film-to-film variations in enzyme coverage on the electrode make quantitative conclusions on the activity less reliable from this method.^[24] The electrochemical results (Figure 2b,c) are generally consistent with the biochemical assay data. Although the interaction between the protein and the electrode is not fully understood and a single amino acid exchange at the enzyme surface (e.g. D467S) might have an impact on immobilisation to the electrode, this is unlikely to be a significant effect due to the high number of protein-electrode interactions of the large SH enzyme. In fact, all variants show lowered current for NAD⁺ reduction, and increased current for NADP⁺ reduction, with the highest NADP⁺ reduction observed for the double variant SH^{E341A/D467S}. The electrochemical measurements also show that the onset potential for NAD(P)⁺ reduction is not significantly affected by the amino acid exchanges. The voltammogram recorded at the electrode modified with SH^{D467S} shows a slight redox peak at approximately -250 mV; this is likely due to dissociated FMN adhering to the electrode,^[24] suggesting increased flavin loss by this variant.

We then determined the Michaelis-Menten parameters for NAD(P)⁺ reduction for the SH enzymes. The results clearly show that all the exchanges significantly increased the affinity of SH for NADP⁺ (Table 1). Even the D467S variant, with a less than 2-fold increase in k_{cat} for NADP⁺ reduction compared to native SH, already showed a $K_{\text{M}}^{\text{NADP}}$ of 3.4 mM, supporting the previous observation that remote alterations can affect the NAD(P)H binding properties of the catalytic centre.^[35] The E341A exchange led to an increase of $K_{\text{M}}^{\text{NAD}}$ and a concomitant loss of NAD⁺ reduction activity (Figure 2a,b), presumably due to insufficient substrate stabilisation as the hydrogen bond between the E341 side chain and the 2'-hydroxyl group of the adenosine ribose of NAD⁺ is lost (Figure 1c,d). On the other hand, the much smaller alanine side chain provides enough space for the additional 2'-phosphate group of NADP⁺, which becomes accepted as a substrate with a K_{M} of 4.8 mM (Table 1); the k_{cat} of 3.3 s⁻¹ is more than 30-fold higher than for native SH (Figure 2a,c). An additive effect was achieved by combining the E341 A and D467S exchanges, with the SH^{E341A/D467S} variant

Table 1. K_M and k_{cat} values for H_2 -driven NAD^+ and $NADP^+$ reduction by SH variants.

SH variant	$NAD^+ \rightarrow NADH^{[a]}$ K_M [mM]	k_{cat} [s^{-1}]	k_{cat}/K_M [s^{-1}/mM]	$NADP^+ \rightarrow NADPH$ K_M [mM]	k_{cat} [s^{-1}]	k_{cat}/K_M [s^{-1}/mM]
native	0.55 ± 0.08	690 ± 63	1255	> 50	< 0.1	< 0.01
E341A	0.61 ± 0.11	20 ± 2.6	32.6	4.8 ± 1.7	3.3 ± 1.0	0.68
D467S	0.66 ± 0.18	55 ± 6.9	83.0	3.4 ± 1.0	0.2 ± 0.04	0.06
E341A/D467S	0.65 ± 0.18	68 ± 7.4	36.9	2.3 ± 1.1	8.5 ± 1.6	3.7
E341A/S342R	1.32 ± 0.29	25 ± 4	18.9	0.60 ± 0.33	6.0 ± 0.4	9.9

[a] Values were determined biochemically using 2 biological replicates for SH, SH^{E341A}, and SH^{D467S} and 3 biological replicates for the variant SH proteins carrying double exchanges. Conditions: 740 μM H_2 , 0.1–6 mM $NAD(P)^+$, approx. 40 nM enzyme in 25 mM Tris–HCl, pH 8.0 at 30 °C. Data are given as mean \pm SD.

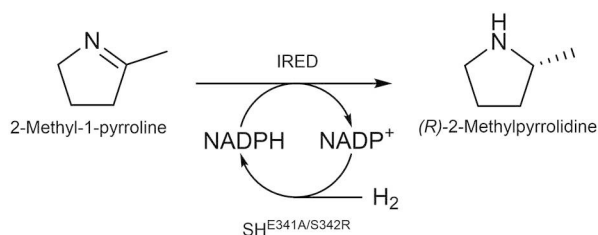
showing a K_M^{NADP} of 2.3 mM and k_{cat} of $8.5 s^{-1}$. Even more specific binding of $NADP^+$ ($K_M^{NADP} = 0.6$ mM) was observed upon introduction of the S342R exchange to the SH^{E341A} variant although the k_{cat} was slightly lowered to $6.0 s^{-1}$ (Table 1). The positively charged side chain of Arg342 is proposed to form hydrogen bonds to the 2'-phosphate group of $NADP^+$.^[36] The highest catalytic efficiency of the SH^{E341A/S342R} variant for H_2 -driven $NADP^+$ reduction and the lowest for NAD^+ reduction are consistent with this proposal. Thus, the cofactor preference of SH was switched by just two exchanges in the SH^{E341A/S342R} variant.

H_2 -driven NADPH recycling for the reduction of cyclic imines

The most promising variant, SH^{E341A/S342R}, showed good activity for both H_2 -driven ($k_{cat} = 6.0 s^{-1}$) and electrode-driven $NADP^+$ reduction and had an acceptable Michaelis constant of 600 μM for $NADP^+$. These properties made it an attractive candidate to

investigate H_2 -driven regeneration of NADPH to support the activity of redox enzymes such as imine reductases. We chose an imine reductase (IREd) that catalyses the asymmetric reduction of 2-methyl-1-pyrroline to a single enantiomer of 2-methylpyrrolidine (Scheme 1).

The efficiency of the SH^{E341A/S342R} in NADPH cofactor regeneration was demonstrated with four different biotransformations (Table 2, entries 1–4), all of which contained 1 mg IREd and 0.1 mg SH^{E341A/S342R} in a 1 mL-reaction mixture with varying substrate and cofactor concentrations at 2 bar H_2 . Full conversion (> 99%) of 15 mM substrate as starting material was achieved with 1 mM of $NADP^+$ in an overnight reaction (16 h, Table 2, entry 1). An increase of substrate concentration (25 mM) led to a concomitant increase in the total turnover number of the SH (Table 2, entry 2). The highest total turnover number of SH (35000) was obtained with a higher substrate concentration and a prolonged reaction time of 40 h. A still significant conversion of 34% was reached after 40 h with 15 mM substrate and just 0.1 mM of cofactor. Under these conditions, the highest cofactor total turnover number of 51 was achieved. Notably, the enantiomeric excess in all reactions was greater than 99.



Scheme 1. IREd-catalysed conversion of 2-methyl-1-pyrroline into (*R*)-2-methylpyrrolidine. H_2 -driven NADPH recycling is mediated by the SH^{E341A/S342R} protein.

H_2 -driven $NADP^+$ reduction in the presence of O_2

The native SH is well-known for its capacity to maintain its H_2 -dependent NAD^+ reduction activity in the presence of atmospheric O_2 concentrations.^[17,18] To test the effect of the amino acid exchanges on O_2 tolerance, we surveyed the H_2 -driven $NADP^+$ reduction capacity of the SH variants in the presence of

Table 2. H_2 -driven $NADP^+$ reduction by SH^{E341A/S342R} to support an IREd reaction.

Entry ^[a]	[Substrate] [mM]	[Cofactor] [mM]	Time [h]	Conversion [%]	[Product]/ [g · L ⁻¹]	ee	Cofactor TTN	SH TTN
1	15	1	16	99	1.3	99	15	24000
2	25	1	16	67	1.4	99	17	27000
3	25	1	40	88	2.0	99	22	35000
4	15	0.1	40	34	0.4	99	51	8000

[a] reaction conditions: 15–25 mM substrate, 0.1–1 mM $NADP^+$ cofactor, 1 mg (0.04 U) imine reductase, 0.1 mg SH^{E341A/S342R} in 1 mL Tris–HCl (100 mM, pH 8), incubated for 16–40 h at 200 rpm under 2 bar H_2 . See Table S1 for control reactions. The abbreviation “TTN” refers to the total turnover number of 2-methyl-1-pyrrolidine converted per mol of cofactor/enzyme.

0.23 mM O₂, equivalent to the O₂ level in aqueous solution equilibrated in air. The results are shown in Table 3 and clearly demonstrate that the SH variants are active for NADPH regeneration in the presence of this level of O₂. Although the O₂ tolerance was compromised somewhat in the single variants, importantly, the double variants (which are most active for NADP⁺ reduction) showed similar O₂ tolerance compared to native SH.

SH-mediated NADPH recycling for H₂-driven alkane oxidation by P450_{BM3}

The fact that the variant SH^{E341A/S342R} remained catalytically active in the presence of O₂ prompted us to investigate H₂-driven regeneration of NADPH to support the activity of enzymes such as cytochrome P450 monooxygenases, which require O₂ as co-substrate. P450 enzymes catalyse the selective oxidative functionalisation of unactivated C–H bonds to the alcohol functionality – one of the most difficult reactions in classical synthesis. P450-catalysed reactions have huge potential application in synthesis (e.g. for generating drug metabolites and fine chemicals).^[37] All eukaryotic and mitochondrial P450s utilise electrons from NADPH to activate O₂. Whilst the majority of bacterial P450s require NADH, a significant number are NADPH-dependent including P450_{BM3} (CYP102A1) from *Bacillus megaterium*, a highly active, catalytically self-sufficient single-polypeptide enzyme that has been extensively engineered for the oxidation of unnatural substrates.^[13,28,38]

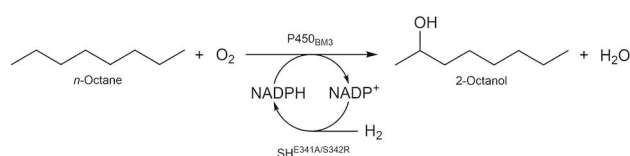
Native P450_{BM3} and its A330P variant were studied for octane oxidation (Scheme 2) with H₂-driven NADPH regeneration with the SH^{E341A/S342R} variant.

The native P450_{BM3} enzyme and the A330P variant produce different ratios of octanols and octanones in air when glucose dehydrogenase (GDH) is used for NADPH regeneration,^[28] and therefore provide a useful test pair for exploring whether the product distribution is perturbed by applying the SH^{E341A/S342R}. A safe mixture of 90% H₂:10% air (i.e. approximately 2% O₂) was selected for this work, and experiments were carried out in air at ambient temperature. We first set out to determine whether 10% air is sufficient to support P450_{BM3} activity by comparing octane oxidation in air versus 10% air in N₂, using GDH/glucose for NADPH regeneration. Both enzymes gave the same product concentrations and distributions, within experimental error, in air and in 10% air in N₂ (Figure S3, Table S2), showing that P450_{BM3} is able to operate under a sub-ambient O₂ partial pressure, as described previously.^[39] Next, we compared octane oxidation for native P450_{BM3} and the A330P variant under 90% H₂:10% air using GDH/glucose or the SH^{E341A/S342R} as the NADPH regeneration system. For each P450_{BM3} enzyme, the total product concentrations and distributions under the different conditions were identical, within experimental error (Figure 3, Table S2). As expected, no product formation was detected in the absence of NADP⁺. We conclude that the O₂-tolerant SH^{E341A/S342R} variant supports H₂-driven NADPH-dependent substrate oxidation by P450_{BM3} using safe H₂/air mixtures as effectively as the GDH/glucose system, under these reaction conditions.

Table 3. Oxygen tolerance of NADP⁺-reducing SH variants.

SH Variant	Condition ^[a]	Hydrogenase activity ^[a] [U · mg ^{−1}]	Hydrogenase activity [%]
SH	−O ₂	53.6 ± 2.3 ^[b]	100
	+O ₂	46.9 ± 0.5 ^[b]	87
SH ^{E341A}	−O ₂	0.78 ± 0.01	100
	+O ₂	0.43 ± 0.01	56
SH ^{D467S}	−O ₂	0.22 ± 0.07	100
	+O ₂	0.10 ± 0.02	46
SH ^{E341A/D467S}	−O ₂	0.93 ± 0.01	100
	+O ₂	0.83 ± 0.01	89
SH ^{E341A/S342R}	−O ₂	1.22 ± 0.01	100
	+O ₂	1.15 ± 0.02	94

[a] H₂-dependent reduction of NAD(P)⁺ was measured biochemically in the presence of either 50% H₂/50% N₂ (−O₂) or 50% H₂/30% N₂/20% O₂ (+O₂), corresponding to 0.23 mM O₂. [b] As there is no NADP⁺ reduction activity detectable for native SH, NAD⁺ was used as the substrate.



Scheme 2. P450_{BM3}-catalysed oxidation of *n*-octane into 2-octanol. H₂-driven NADPH recycling is mediated by the SH^{E341A/S342R} protein.

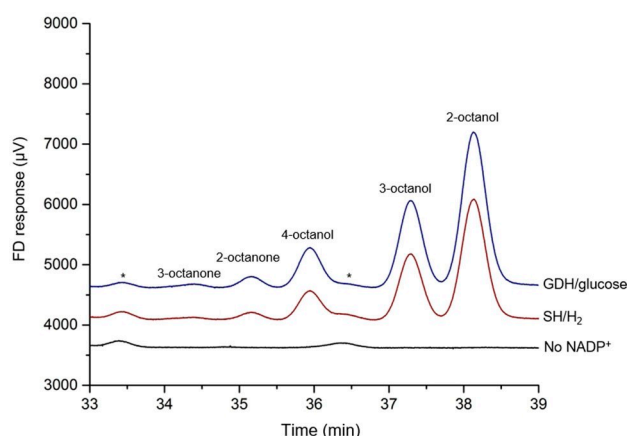


Figure 3. GC analysis of octane oxidation by the A330P variant of P450_{BM3} with different cofactor recycling systems. The total reaction volume was 1.5 mL including 100 mM phosphate buffer, pH 7.4, 0.5 μM P450_{BM3}, 1 mM NADP⁺ (or in black the control reaction without NADP⁺), 5 mM octane, and 20 μg · mL^{−1} bovine liver catalase under 90% H₂:10% air (i.e. 2% O₂) with either, in blue, glucose dehydrogenase (GDH, 10 U · mL^{−1}) and glucose (0.2 M) or, in red, SH^{E341A/S342R} (1 U/mL), for NADPH regeneration. The total integrated areas of the product peaks for the GDH/glucose and SH/H₂ reactions are within 5% of each other. Asterisks denote background contaminant peaks.

Conclusions

Our results show that all of the engineered SH variants catalyse H_2 -dependent $NADP^+$ reduction, which is not the case for native SH. The cofactor preference was switched from NAD^+ to $NADP^+$ in the case of the $SH^{E341A/S342R}$ and $SH^{E341A/D467S}$ proteins, and importantly, these double variants of the SH are still able to oxidise H_2 in the presence of O_2 , with an O_2 -tolerance comparable to the native SH. Notably, a further increase in $NADP^+$ -reducing activity was not achieved with the $SH^{E341A/S342R/D467S}$ variant, which determines the current limit for rational design. Further improvements, however, might be possible by directed evolution using a microorganism with NADPH deficiency, which can be compensated by NADPH-producing SH. Nonetheless, the increased catalytic efficiency for H_2 -driven $NADP^+$ reduction enables H_2 -driven biotransformations with enzyme cascades containing NADPH-dependent oxidoreductases, such as imine reductase and monooxygenase. In fact, the O_2 -tolerant $SH^{E341A/S342R}$ variant supported H_2 -driven NADPH-dependent octane oxidation by cytochrome $P450_{BM3}$ as effectively as the industry standard GDH/glucose system with the advantage of guaranteeing 100% atom efficiency and no generation of carbon-based by-products from the cofactor recycling. The biotransformation was performed with a safe gas mixture containing 2% O_2 and 90% H_2 (remainder N_2). To our knowledge, this is the first demonstration of H_2 -driven NADPH recycling by a hydrogenase in the presence of O_2 . Notably, use of H_2 and other flammable reagents is well established in continuous flow technologies where the continuous addition of low levels of reactant provides for safe operation. Using H_2 as reductant, we have been able to translate biocatalytic reactions into continuous processing,^[40] and this approach would likely enable the O_2 -dependent reactions to be carried out with improved control, safety and productivity. The ability to use H_2 as a reducing agent for NADPH recycling opens up opportunities for highly atom-efficient catalysis by NADPH-dependent enzymes, providing a versatile platform for future biotransformations with NADPH dependent oxidoreductases.

Experimental Section

Genetic construction of SH derivatives

To facilitate mutagenesis of the genes encoding the NAD^+ reductase module, HoxFU, of the *Ralstonia eutropha* SH, a broad-host-range vector harbouring just the *hoxFU* genes under control of the SH promoter was constructed. A 2823-bp XbaI-BamHI fragment was excised from plasmid pJH#2904 and ligated into the vector pCM66 digested with the same restriction endonucleases. The resulting plasmid, pJP66, encodes the N-terminally Strep-tagged HoxF subunit as well as the HoxU protein and served as template for site-directed mutagenesis. Introduction of site-specific mutations was performed by a modified QuikChangeTM protocol.^[41] For the E341A and D467S exchanges in HoxF, primers 5'-ATC TGC GGC GAC gca TCG GCG CTC ATC-3' and 5'-CGC AAG CTC GCG TAC GAA TCG CTT tcg TGC AAT GGC GCC-3', respectively, were used (exchanged bases in lower case letters). Desired nucleotide exchanges in the resulting plasmids, pJP01 and pJP02, respectively,

were confirmed by sequence analysis using primers 5'-GTT ATC GCC GCG TAT GC-3' and 5'-GAT CGA ACG ATG GCA GC-3'. Plasmid pJP01 then served as template to introduce the D467S exchange using the aforementioned primer. The resulting plasmid encoding HoxF^{E341A/D467S}-HoxU was named pJP03. To construct the E341A/S342R double exchange, the primer 5'-CTT ATA TCT GCG GCG ACG CAC gc G CGC TCA TCG AGT CCT GCG-3' was designed and used with pJP1 to yield pJP04. Plasmid pJP04, in turn, served as the template to introduce a further D467S exchange by employing primer 5'-CGC AAG CTC GCG TAC GAA tcg CTT TCG TGC AAT GGC GCC-3'. This yielded plasmid pJP5 encoding HoxF^{E341A/S342R/D467S}. Plasmids pJP66 and pJP01-05 were transferred via conjugation from *E. coli* S17-1 to *Ralstonia eutropha* strain HF903,^[24] which carries in-frame deletions in *hoxFU* and the large subunits, *hoxG* and *hoxC*, of the membrane-bound (MBH) and regulatory hydrogenase (RH), respectively. Thus, this strain is SH-, MBH- and RH-negative but possesses all other genes that are necessary for hydrogenase maturation.

Production and purification of $NADP^+$ -reducing SH derivatives

R. eutropha HF903 transconjugants carrying either of pJP66 and pJP01-04 were grown heterotrophically in a mineral salts medium containing a mixture of 0.05% (w/v) fructose and 0.4% (v/v) glycerol (FGN medium) at 30 °C until the optical density at 436 nm was 9–11.^[42] Cells were harvested by centrifugation at 11,500 × g for 15 min at 4 °C. The cell pellets were resuspended in 50 mM Tris-HCl, pH 8, containing 150 mM KCl, 5% (v/v) glycerol, 5 mM NAD^+ and protease-inhibitor cocktail (EDTA-free Protease Inhibitor, Roche). After two passages through a chilled French press cell at 18,000 psi, debris was separated from the soluble extract by centrifugation at approx. 140,000 × g for 45 min. The supernatant was loaded onto 2 mL Strep-Tactin Superflow columns (IBA), which were previously equilibrated with resuspension buffer. After washing with at least 6 column-volumes of resuspension buffer the protein was eluted in resuspension buffer containing 5 mM desthiobiotin. A final concentration of 2–6 mg mL⁻¹ of purified protein was achieved using Ultra Centrifugal Filter Units (Amicon). From 1 g of cell mass (wet weight), we usually obtained 1 mg of purified SH. The protein concentration was determined according to the method of Bradford.^[43]

Hydrogenase activity measurements

H_2 -dependent $NAD(P)^+$ reduction activities were determined as described previously.^[44] The reaction was performed in rubber-sealed cuvettes filled with 2 mL of 50 mM Tris-HCl, pH 8.0, 1 mM $NAD(P)^+$, 1 mM DTT, and 1 μ M FMN. The solution was flushed with H_2 , and the reaction was started by adding 2–5 μ L of purified protein. The absorbance change through accumulation of $NAD(P)H$ was measured at 340 nm with a Cary 50 (Varian) spectrophotometer. For determination of Michaelis-Menten parameters, initial reaction velocities at varying $NAD(P)^+$ concentrations were recorded. The velocities were plotted against substrate concentrations and fitted to the Michaelis-Menten equation using Origin 9.1. Activity tests in the presence of O_2 were performed in rubber-sealed cuvettes containing appropriate mixtures of gas-saturated (H_2 , N_2 , and O_2) buffers.^[18]

Electrochemical activity measurements

Electrochemical experiments were performed following previously described procedures^[24] in an anaerobic glove box (mBraun, $O_2 < 0.1$ ppm) using an Autolab potentiostat (EcoChemie 128N). The

pyrolytic graphite edge rotating disc electrode (RDE) with planar electrode surface area of 0.03 cm^2 was prepared 'in house', and was rotated at 2000 rpm for all experiments using an EG&G electrode rotator model 636 to ensure efficient mass transport of substrate and product to and from the enzyme films. Before each scan the electrode was polished using a slurry of $1\text{ }\mu\text{m}$ alumina, and was sonicated in purified water (MilliQ , $18\text{ M}\Omega\cdot\text{cm}$) for 10 s. The electrode was then rinsed and dried before application of an enzyme film by spotting enzyme ($0.5\text{ }\mu\text{L}$) onto the electrode and leaving it to adsorb over ~ 20 seconds. The electrode was then placed into buffered electrolyte (100 mM Tris-HCl buffer, pH 8.0) containing 5 mM cofactor. Cyclic voltammograms were recorded at a scan rate of $10\text{ mV}\cdot\text{s}^{-1}$. The reference electrode was a saturated calomel electrode (SCE, BAS) and potentials were converted to units of Volts (V) vs. SHE using $E(\text{SHE}) = E(\text{SCE}) + 0.242\text{ V}$ at 25°C . The counter electrode was a Pt wire.

H_2 -driven IRED reaction

Reaction mixtures with a total volume of 1 mL consisted of H_2 saturated Tris-HCl buffer (100 mM, pH 7.5), $0.1\text{--}1\text{ mM}$ NADP^+ , $1.3\text{--}2\text{ g}\cdot\text{L}^{-1}$ substrate, $1\text{ mg}\cdot\text{mL}^{-1}$ IRED (Prozomix Ltd., PRO-CoE-IRED (046)) and $0.11\text{ mg}\cdot\text{mL}^{-1}$ $\text{SH}^{\text{E341A/S342R}}$ variant ($1\text{ U}\cdot\text{mg}^{-1}$). These were prepared in a stainless steel pressure vessel (Tinyclave steel, Büchi AG) fitted with a 50 mL glass insert equipped with a magnetic stirrer bar and sealed in a H_2 atmosphere (2 bar). The reaction mixtures were stirred (200 rpm) at 32°C for 16–40 h and aliquots were removed at the end point for analysis by GC and ^1H NMR.

Control reactions (Table S1) were performed on a 1 mL scale in round bottom flasks (10 mL) and included a magnetic stirrer bar. Initially, reaction mixtures consisting of 1 mM NAD(P)^+ in Tris-HCl buffer (100 mM, pH 8.0) were saturated with H_2 , and then SH or SH variant (to a concentration $0.11\text{ mg}\cdot\text{mL}^{-1}$, 0.11 U) was added. After 5 minutes, IRED was added ($100\text{ }\mu\text{L}$ from $10\times$ concentrated stock solution, $1\text{ mg}\cdot\text{mL}^{-1}$, 0.04 U). After a further 5 min, substrate was added (2-methyl-1-pyrroline, 25 mM) and the reaction was stirred at 200 rpm. The end solution was analysed by GC and ^1H NMR.

Glucose dehydrogenase (GDH) control reactions were performed on a 1 mL scale in capped glass vials (2 mL) and stirred with a magnetic stirrer bar. The reaction was initiated by addition of 1 mg of GDH (Codexis, GDH-105) and 1 mg of IRED (both added as $100\text{ }\mu\text{L}$ from $10\times$ concentrated stock solutions) to a solution of 1 mM NADP^+ , 20 mM glucose, and 5 mM imine in Tris-HCl (100 mM, pH 8.0) and stirred at 200 rpm overnight. The end solution was analysed by ^1H NMR.

Gas chromatography for IRED reaction

Following the IRED reactions described above, a $100\text{ }\mu\text{L}$ aliquot of the solution was basified by addition of $10\text{ }\mu\text{L}$ of 10 N NaOH. The resulting solution was extracted by addition of $200\text{ }\mu\text{L}$ EtOAc (containing 2 mM undecane as internal standard), then centrifuged at $10,000\times g$ for 3 min. The organic layer was dried over MgSO_4 , then centrifuged at $10,000\times g$ for 3 min. Subsequently, $100\text{ }\mu\text{L}$ of the dried organic layer was heated to 60°C with $15\text{ }\mu\text{L}$ of acetic anhydride and $7\text{ }\mu\text{L}$ of pyridine for 1 h in a capped glass GC vial. The resulting solution was analysed by chiral GC-FID (Figures S4–S6) using an Agilent CP-Chirasil-Dex CB column (25 m length, 0.25 mm diameter, $0.25\text{ }\mu\text{m}$ film thickness), fitted with a guard of 10 m deactivated fused silica of the same diameter. Carrier gas: He (CP grade), $2\text{ mL}\cdot\text{min}^{-1}$ (constant flow). Inlet temperature = 200°C . Injection volume = $0.1\text{ }\mu\text{L}$. See also parameters in Table 4.

NMR spectroscopy for IRED reaction

All NMR spectroscopy was carried out on a Bruker Avance III HD nanobay (400 MHz) or a Bruker Avance III HD (500 MHz) (Figures S7–S10). Following removal of denatured enzyme by centrifugation, $450\text{ }\mu\text{L}$ of the sample solution was transferred to a Norell® SelectSeries™ 5 mm 400 MHz sample tube. A further $50\text{ }\mu\text{L}$ of D_2O was added for field locking.

H_2 -driven octane oxidation by P450_{BM3}

A mixture with a total volume of 1.5 mL consisting of 100 mM phosphate buffer, pH 7.4, $0.5\text{ }\mu\text{M}$ P450_{BM3} enzyme, 1 mM NADP^+ , $20\text{ }\mu\text{g}\cdot\text{mL}^{-1}$ catalase, and $100\text{ }\mu\text{L}$ of a solution of the $\text{SH}^{\text{E341A/S342R}}$ variant (NAD^+ reduction activity = $1\text{ nmol}\cdot\text{min}^{-1}\cdot\mu\text{L}^{-1}$) was prepared in a 6 mL ($23\times 38\text{ mm}$) glass vial in a glove box. O_2 was removed from all the solutions, and the phosphate buffer was saturated with H_2 for 30 min before being taken into the glove box. The glass vial was sealed with a suba seal, and the reaction mixture was bubbled with H_2 for a further 30 s and H_2 was flushed into the headspace for 15 seconds. The sealed glass vial was taken out of the glove box and octane was added as a 0.2 M stock in DMSO to a final concentration of 5 mM using a gas-tight syringe. The glass vial was then injected with 10% air to give 2% O_2 overall in both the solution and the headspace. The vial, with the suba seal in place, was wrapped in Parafilm to minimise gas loss. The reaction mixture was stirred for 2 h at ambient temperature, after which a 1 mL aliquot was removed and extracted with $300\text{ }\mu\text{L}$ ethyl acetate. After vortex mixing and centrifugation ($14,333\times g$) for 2 min, the organic layer was removed and analysed by gas chromatography on a TRACE GC instrument (ThermoFinnigan) with a SPB-1 fused silica capillary column ($60\text{ m}\times 0.53\text{ mm}$ i.d. and $1\text{ }\mu\text{m}$ film thickness) and flame ionization detection. Helium was used as the carrier gas (flow rate $3.5\text{ mL}\cdot\text{min}^{-1}$). The injector was at 230°C and the FID at 250°C . The oven temperature was held at 100°C for 40 min; the retention times were: 3-octanone, 34.4 min; 2-octanone, 35.2 min; 4-octanol, 35.9 min; 3-octanol, 37.3 min; 2-octanol, 38.1 min. For the reactions under 10% air and with GDH/glucose as the NADPH regeneration system, the mixtures contained $10\text{ U}\cdot\text{mL}^{-1}$ GDH and 0.2 M glucose in place of the SH variant. Such high concentration of glucose is used in order to ensure that cofactor recycling is not limiting the reaction. Control reactions included mixtures without NADP^+ but under 2% O_2 , and those using GDH/glucose for NADPH regeneration in air.

Acknowledgements

We are indebted to Janna Schoknecht for skilful assistance. Research by J.P., L.L. and O.L. was funded by the Deutsche Forschungsgemeinschaft (DFG, German Research Foundation) under Germany's Excellence Strategy – EXC 2008–390540038 – UniSysCat., and the research project 405325648 (to L.L.). Research by H.A.R. and K.A.V. was supported by an industry interaction voucher from the Metals in Biology BBSRC NIBB BB/L013711/1, and by EPSRC IB Catalyst award EP/N013514/1, which also supported J.N.. K.U. was supported by EPSRC DTA studentship, 2012, EP/K503113/1, and J.P. was supported by a scholarship from the Berlin International Graduate School for Natural Science & Engineering (BIG-NSE). Open access funding enabled and organized by Projekt DEAL.

Conflict of Interest

The authors declare no conflict of interest.

Keywords: hydrogenase · metalloenzyme · cytochrome P450 · monooxygenase · oxidoreductase · imine reductase · octane oxidation · nicotinamide cofactor · NADH, NADPH · cofactor recycling · biotransformation

- [1] a) A. Liese, M. V. Filho, *Curr. Opin. Biotechnol.* **1999**, *10*, 595; b) A. J. J. Straathof, S. Panke, A. Schmid, *Curr. Opin. Biotechnol.* **2002**, *13*, 548; c) B. M. Nestl, B. A. Nebel, B. Hauer, *Curr. Opin. Biotechnol.* **2011**, *15*, 187; d) D. J. Pollard, J. M. Woodley, *Trends Biotechnol.* **2007**, *25*, 66.
- [2] a) D. Muñoz Solano, P. Hoyos, M. J. Hernáiz, A. R. Alcántara, J. M. Sánchez-Montero, *Bioresour. Technol.* **2012**, *115*, 196; b) W. Kroutil, H. Mang, K. Edegger, K. Faber, *Curr. Opin. Chem. Biol.* **2004**, *8*, 120.
- [3] R. Bernhardt, V. B. Urlacher, *Appl. Microbiol. Biotechnol.* **2014**, *98*, 6185.
- [4] C.-H. Wong, G. M. Whitesides, *J. Am. Chem. Soc.* **1981**, *103*, 4890.
- [5] a) J. M. Vrtis, A. K. White, W. W. Metcalf, W. A. van der Donk, *Angew. Chem. Int. Ed.* **2002**, *41*, 3257; b) E. Keinan, E. K. Hafeli, K. K. Seth, R. Lamed, *J. Am. Chem. Soc.* **1986**, *108*, 162.
- [6] K. Hoelsch, I. Sührer, M. Heusel, D. Weuster-Botz, *Appl. Microbiol. Biotechnol.* **2013**, *97*, 2473.
- [7] a) D. Holtmann, M. W. Fraaije, I. W. C. E. Arends, D. J. Opperman, F. Hollmann, *Chem. Commun.* **2014**, *50*, 13180; b) L. Lauterbach, O. Lenz, K. A. Vincent, *FEBS J.* **2013**, *280*, 3058.
- [8] a) L. Greiner, I. Schröder, D. H. Müller, A. Liese, *Green Chem.* **2003**, *5*, 697; b) R. Mertens, L. Greiner, E. C. D. van den Ban, H. B. C. M. Haaker, A. Liese, *J. Mol. Catal. B Enzym* **2003**, *24–25*, 39; c) R. Mertens, A. Liese, *Curr. Opin. Biotechnol.* **2004**, *15*, 343; d) J. Ratzka, L. Lauterbach, O. Lenz, M. B. Ansorge-Schumacher, *J. Mol. Catal. B* **2012**, *74*, 219.
- [9] J. Ratzka, L. Lauterbach, O. Lenz, M. B. Ansorge-Schumacher, *Biocatal. Biotransform.* **2011**, *29*, 246.
- [10] C.-H. Wu, P. M. McTernan, M. E. Walter, M. W. W. Adams, *Archaea* **2015**, *2015*, 912582.
- [11] P. Kwan, C. L. McIntosh, D. P. Jennings, R. C. Hopkins, S. K. Chandrayan, C.-H. Wu, M. W. W. Adams, A. K. Jones, *J. Am. Chem. Soc.* **2015**, *137*, 13556.
- [12] a) S. G. Bell, X. Chen, F. Xu, Z. Rao, L.-L. Wong, *Biochem. Soc. Trans.* **2003**, *31*, 558; b) C. F. Harford-Cross, A. B. Carmichael, F. K. Allan, P. A. England, D. A. Rouch, L. L. Wong, *Protein Eng.* **2000**, *13*, 121; c) L. L. Wong, *Curr. Opin. Chem. Biol.* **1998**, *2*, 263.
- [13] C. J. C. Whitehouse, S. G. Bell, L.-L. Wong, *Chem. Soc. Rev.* **2012**, *41*, 1218.
- [14] a) A. K. Holzer, K. Hiebler, F. G. Mutti, R. C. Simon, L. Lauterbach, O. Lenz, W. Kroutil, *Org. Lett.* **2015**, *17*, 2431; b) H. A. Reeve, L. Lauterbach, O. Lenz, K. A. Vincent, *ChemCatChem* **2015**, *7*, 3480; c) H. A. Reeve, L. Lauterbach, P. A. Ash, O. Lenz, K. A. Vincent, *Chem. Commun.* **2011**, *48*, 1589.
- [15] T. H. Lonsdale, L. Lauterbach, S. Honda Malca, B. M. Nestl, B. Hauer, O. Lenz, *Chem. Commun.* **2015**, *51*, 16173.
- [16] P. Vandamme, T. Coenye, *Int. J. Syst. Evol. Microbiol.* **2004**, *54*, 2285.
- [17] K. Schneider, H. G. Schlegel, *Biochem. J.* **1981**, *193*, 99.
- [18] L. Lauterbach, O. Lenz, *J. Am. Chem. Soc.* **2013**, *135*, 17897.
- [19] a) T. Burgdorf, E. van der Linden, M. Bernhard, Q. Y. Yin, J. W. Back, A. F. Hartog, A. O. Muijsers, C. G. de Koster, S. P. J. Albracht, B. Friedrich, *J. Bacteriol.* **2005**, *187*, 3122; b) K. Schneider, H. G. Schlegel, *Biochim. Biophys. Acta* **1976**, *452*, 66.
- [20] J. T. Wu, L. H. Wu, J. A. Knight, *Clin. Chem.* **1986**, *32*, 314.
- [21] N. S. Scrutton, A. Berry, R. N. Perham, *Nature* **1990**, *343*, 38.
- [22] J. K. B. Cahn, C. A. Werlang, A. Baumschlager, S. Brinkmann-Chen, S. L. Mayo, F. H. Arnold, *ACS Synth. Biol.* **2017**, *6*, 326.
- [23] a) S. J. Pilkington, J. M. Skehel, R. B. Gennis, J. E. Walker, *Biochemistry* **1991**, *30*, 2166; b) R. G. Efremov, L. A. Sazanov, *Curr. Opin. Struct. Biol.* **2011**, *21*, 532.
- [24] L. Lauterbach, Z. Idris, K. A. Vincent, O. Lenz, *PLoS One* **2011**, *6*, e25939.
- [25] M. Horsch, L. Lauterbach, O. Lenz, P. Hildebrandt, I. Zebger, *FEBS Lett.* **2012**, *586*, 545.
- [26] K. Morina, M. Schulte, F. Hubrich, K. Dorner, S. Steimle, S. Stolpe, T. Friedrich, *J. Biol. Chem.* **2011**, *286*, 34627.
- [27] A. Lerchner, A. Jarasch, W. Meining, A. Schiefner, A. Skerra, *Biotechnol. Bioeng.* **2013**, *110*, 2803.
- [28] C. J. C. Whitehouse, S. G. Bell, H. G. Tufton, R. J. P. Kenny, L. C. I. Ogilvie, L.-L. Wong, *Chem. Commun.* **2008**, 966.
- [29] Y. Shomura, M. Taketa, H. Nakashima, H. Tai, H. Nakagawa, Y. Ikeda, M. Ishii, Y. Igarashi, H. Nishihara, K.-S. Yoon, et al., *Science* **2017**, *357*, 928.
- [30] J. M. Berrisford, L. A. Sazanov, *J. Biol. Chem.* **2009**, *284*, 29773.
- [31] L. A. Sazanov, P. Hinchliffe, *Science* **2006**, *311*, 1430.
- [32] R. Takase, A. Ochial, B. Mikami, W. Hashimoto, K. Murata, *Biochim. Biophys. Acta* **2010**, *1804*, 1925.
- [33] O. Schmitz, G. Boison, H. Salzmann, H. Bothe, K. Schutz, S.-H. Wang, T. Happe, *Biochim. Biophys. Acta* **2002**, *1554*, 66.
- [34] P. Hinchliffe, L. A. Sazanov, *Science* **2005**, *309*, 771.
- [35] E. Aubert-Jousset, M. Cano, G. Guedeney, P. Richaud, L. Courmac, *FEBS J.* **2011**, *278*, 4035.
- [36] O. Carugo, P. Argos, *Proteins* **1997**, *28*, 10.
- [37] F. P. Guengerich, *Nat. Rev. Drug Discovery* **2002**, *1*, 359.
- [38] a) Z. J. Wang, H. Renata, N. E. Peck, C. C. Farwell, P. S. Coelho, F. H. Arnold, *Angew. Chem. Int. Ed. Engl.* **2014**, *53*, 6810; b) G. Di Nardo, V. Dell'Angelo, G. Catucci, S. J. Sadeghi, G. Gilardi, *Arch. Biochem. Biophys.* **2016**, *602*, 106; c) J. A. Dietrich, Y. Yoshikuni, K. J. Fisher, F. X. Wooldard, D. Ockey, D. J. McPhee, N. S. Renninger, M. C. Y. Chang, D. Baker, J. D. Keasling, *ACS Chem. Biol.* **2009**, *4*, 261.
- [39] S. Castrignanò, G. Di Nardo, S. J. Sadeghi, G. Gilardi, *J. Inorg. Biochem.* **2018**, *188*, 9.
- [40] C. Zor, H. A. Reeve, J. Quinson, L. A. Thompson, T. H. Lonsdale, F. Dillon, N. Grobert, K. A. Vincent, *Chem. Commun.* **2017**, *53*, 9839.
- [41] T. Pfirrmann, A. Lokapally, C. Andreasson, P. Ljungdahl, T. Hollemann, *PLoS One* **2013**, *8*, e64870.
- [42] E. Schwartz, U. Gerischer, B. Friedrich, *J. Bacteriol.* **1998**, *180*, 3197.
- [43] M. M. Bradford, *Anal. Biochem.* **1976**, *72*, 248.
- [44] T. Burgdorf, O. Lenz, T. Buhrke, E. van der Linden, A. K. Jones, S. P. Albracht, B. Friedrich, *J. Mol. Microbiol. Biotechnol.* **2005**, *10*, 181.

Manuscript received: May 4, 2020

Revised manuscript received: June 12, 2020

Accepted manuscript online: June 16, 2020

Version of record online: August 10, 2020